Spectral Response and Contact of the Unitary Fermi Gas

Biswaroop Mukherjee, Parth B. Patel, Zhenjie Yan, Richard J. Fletcher, Julian Struck, and Martin W. Zwierlein

Phys. Rev. Lett. **122**, 203402 — Published 23 May 2019

DOI: 10.1103/PhysRevLett.122.203402

Spectral response and contact of the unitary Fermi gas

Biswaroop Mukherjee,[1] Parth B. Patel,[1] Zhenjie Yan,[1]
Richard J. Fletcher,[1] Julian Struck,[1,2] and Martin W. Zwierlein[1]

[1] *MIT-Harvard Center for Ultracold Atoms, Research Laboratory of Electronics, and Department of Physics, Massachusetts Institute of Technology, Cambridge, Massachusetts 02139, USA*
[2] *Département de Physique, Ecole Normale Supérieure / PSL Research University, CNRS, 24 rue Lhomond, 75005 Paris, France*

We measure radiofrequency (rf) spectra of the homogeneous unitary Fermi gas at temperatures ranging from the Boltzmann regime through quantum degeneracy and across the superfluid transition. For all temperatures, a single spectral peak is observed. Its position smoothly evolves from the bare atomic resonance in the Boltzmann regime to a frequency corresponding to nearly one Fermi energy at the lowest temperatures. At high temperatures, the peak width reflects the scattering rate of the atoms, while at low temperatures, the width is set by the size of fermion pairs. Above the superfluid transition, and approaching the quantum critical regime, the width increases linearly with temperature, indicating non-Fermi-liquid behavior. From the wings of the rf spectra, we obtain the contact, quantifying the strength of short-range pair correlations. We find that the contact rapidly increases as the gas is cooled below the superfluid transition.

PACS numbers: 03.75.Ss, 05.30.Fk, 51.30.+i, 71.18.+y

Understanding fermion pairing and pair correlations is of central relevance to strongly interacting Fermi systems such as nuclei [1, 2], ultracold gases [3–6], liquid ^{3}He [7], high temperature superconductors [8], and neutron stars [9]. Strong interactions on the order of the Fermi energy challenge theoretical approaches, especially methods that predict dynamic properties such as transport or the spectral response at finite temperature [10]. Atomic Fermi gases at Feshbach resonances realize a paradigmatic system where the gas becomes as strongly interacting as allowed by unitarity [3–6, 11]. Here, the system becomes universal, requiring only two energy scales: the Fermi energy E_F and thermal energy k_BT, where k_B is the Boltzmann constant and T is the temperature. The corresponding length scales are the interparticle spacing $\lambda_F = n^{-1/3}$ and the thermal de Broglie wavelength $\lambda_T = h/\sqrt{2\pi m k_B T}$, where m and n are the mass and number density of the atoms respectively. When the two energy scales are comparable, the system enters a quantum critical regime separating the high temperature Boltzmann gas from the fermionic superfluid [12]. Quantum criticality is often associated with the absence of quasiparticles [10, 12, 13], spurring a debate on the applicability of Fermi liquid theory to the degenerate normal fluid below the Fermi temperature $T_F = E_F/k_B$ but above the superfluid transition temperature $T_c \approx 0.167\,T_F$ [14–16]. It has been conjectured that preformed pairs exist above T_c, up to a pairing temperature T^* [3, 5, 11, 17–21].

Radiofrequency (rf) spectroscopy measures the momentum integrated, occupied spectral function, providing a powerful tool to study interactions and correlations in Fermi gases [22–27]. Here, a particle is ejected from the interacting many-body state and transferred into a weakly interacting final state. Shifts in rf spectra indicate attractive or repulsive interactions in the gas. At high temperatures, the width of the rf spectrum reflects the scattering rate in the gas, while at low temperatures, the width has been used to infer the pair size of superfluid fermion pairs [26].

The high frequency tails of the rf spectra are sensitive to the spectral function at high momenta, and therefore are governed by short range correlations quantifed by the contact, which also determines the change of the energy with respect to the interaction strength [28–30]. From the momentum distribution within nuclei [1, 2] to the frequency dependence of the shear viscosity in ultracold fermionic superfluids [31, 32], the contact is central to Fermi gases dominated by short-range interactions. Since the contact is proposed to be sensitive to the superfluid pairing gap, it could signal a pseudogap regime above T_c [32–35]. Although the temperature dependence of the contact near T_c has been the subject of many theoretical predictions, a consensus has not been reached [32, 36–38].

Initial studies of unitary Fermi gases using rf spectroscopy were affected by inhomogeneous densities in harmonic traps, yielding doubly-peaked spectra that were interpreted as observations of the pairing gap [25, 46], and from the influence of interactions in the final state, which caused significantly narrower spectra and smaller shifts than expected [22, 46–48]. Measurements of the contact, made using both rf [49, 50] and Bragg [51–53] spectroscopy, were also broadened by inhomogeneous potentials. To avoid trap broadening, tomographic techniques have been used to measure local rf spectra, yielding measurements of the superfluid gap [54], the spectral function [17, 18], and the contact [55]. A recent advance has been the creation of uniform box potentials [56–58]. These are ideal for rf spectroscopy and precision measurements of the contact: since the entire cloud is at a constant density, global probes such as rf address all atoms, and benefit from a stronger signal.

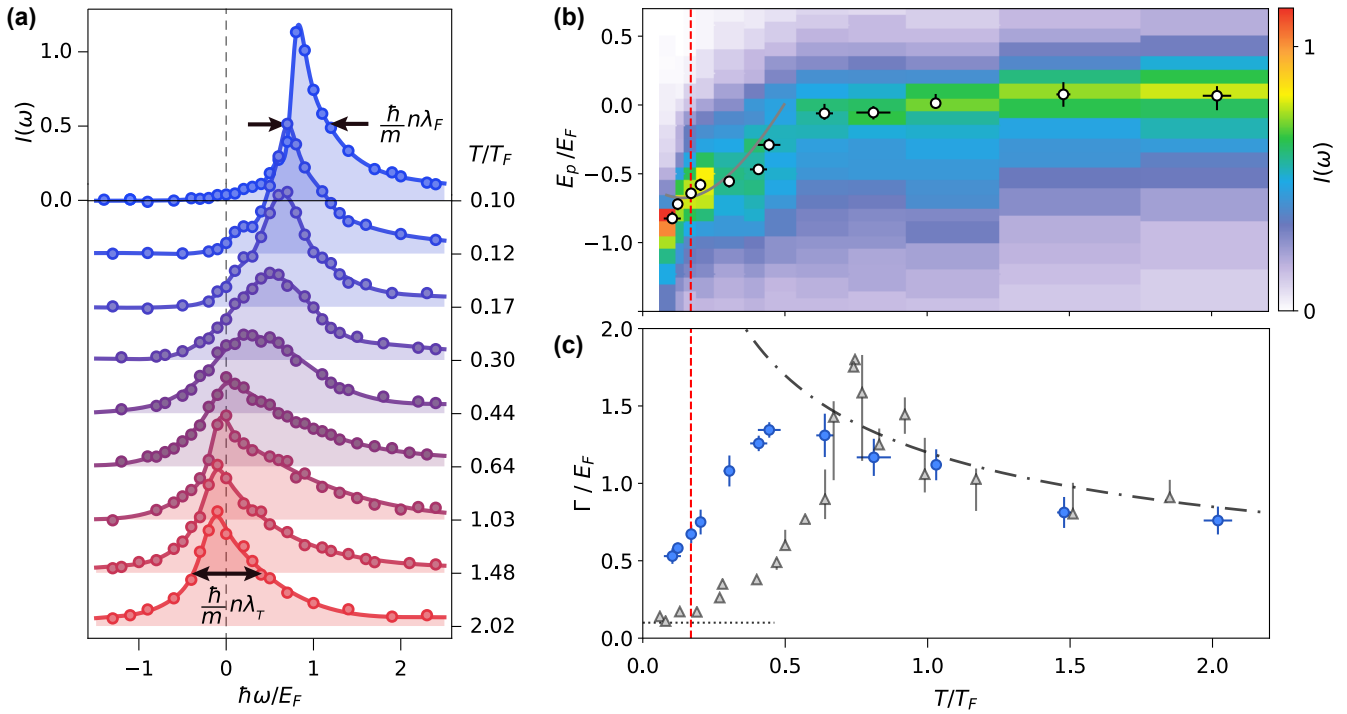

FIG. 1. (a) Thermal evolution of rf spectra. The Rabi frequency is $\Omega_R = 2\pi \times 0.5$ kHz and the pulse duration is $T_{\rm Pulse} = 1$ ms. The solid lines are guides to the eye. (b) Frequency of the peak ($E_p = -\hbar\omega$) of the rf spectra as a function of temperature shown as white dots on an intensity plot of the rf response. The grey solid line is a solution to the Cooper problem at nonzero temperature [39]. (c) The full width at half maximum Γ of the rf peak as a function of T/T_F. The black dot-dashed line $\Gamma/E_F = 1.2\sqrt{T_F/T}$ shows the temperature dependence of the width due to scattering in the high-temperature gas [32, 44]. The grey triangles are the corresponding width measurements of a highly spin-imbalanced gas [45]. The horizontal black dotted line represents the Fourier broadening of $0.1\,E_F$ [39]. The vertical dashed red line in both (b) and (c) marks the superfluid transition [14].

In this letter, we report on rf spectroscopy of the homogeneous unitary Fermi gas in a box potential. A single peak is observed for all temperatures from the superfluid regime into the high temperature Boltzmann gas. The tails of the rf spectra reveal the contact, which shows a rapid rise as the temperature is reduced below T_c.

We prepare ^{6}Li atoms in two of the three lowest hyperfine states $|\downarrow\rangle = |1\rangle$ and $|\uparrow\rangle = |3\rangle$ at a magnetic field of 690 G, where interspin interactions are resonant. A uniform optical box potential with cylindrical symmetry is loaded with $N \sim 10^6$ atoms per spin state (with Fermi energies $E_F \sim h \times 10$ kHz), creating spin-balanced homogeneous gases at temperatures ranging from $T/T_F = 0.10$ to 3.0 [57]. A square rf pulse transfers atoms from state $|\downarrow\rangle$ into state $|f\rangle = |2\rangle$. Final state interactions between atoms in state $|f\rangle$ and atoms in states $|\uparrow\rangle$ and $|\downarrow\rangle$ are small ($k_F a_f \lesssim 0.2$, where a_f is the scattering length characterizing collisions between atoms in the final and initial states, and $\hbar k_F = \sqrt{2mE_F}$ is the Fermi momentum) [26]. After the RF pulse, we measure the atom numbers $N_\downarrow$ and N_f in the initial and final states. Within linear response, according to Fermi's Golden Rule, N_f is proportional to the pulse time $T_{\rm Pulse}$, the square of the single-particle Rabi frequency Ω_R and an energy density of states. We thus define a normalized, dimensionless rf spectrum as $I(\omega) = (N_f(\omega)/N_\downarrow)(E_F/\hbar\Omega_R^2 T_{\rm Pulse})$ [39, 45]. Due to the scale invariance of the balanced unitary Fermi gas, this dimensionless function can only depend on T/T_F and $\hbar\omega/E_F$.

For thermometry, we release the cloud from the uniform potential into a harmonic trap along one direction [45]. Since the cloud expands isoenergetically, the resulting spatial profile after thermalization provides the energy per particle, which can be related to the reduced temperature, T/T_F, using a virial relation and the measured equation of state [14]. To clearly identify the superfluid transition, we measure the pair momentum distribution by a rapid ramp of the magnetic field to the molecular side of the Feshbach resonance before releasing the gas into a harmonic trap for a quarter period [39, 57].

We initially focus on changes in the lineshape for rf frequencies within $\sim E_F/\hbar$ of the bare (single-particle) resonance (see Fig 1(a)), and follow the changes in the peak position E_p (shown in Fig 1(b)). As the hot spin-balanced Fermi gas is cooled below the Fermi temperature, the peak shift decreases from roughly zero for temperatures

$T \gtrsim T_F$, to $E_p \approx -0.8\ E_F$ for temperatures below the superfluid transition temperature (see Fig. 1(b)). At high temperatures, one might naïvely expect a shift on the order of $E_p \sim \hbar n \lambda_T / m$ due to unitarity-limited interactions in the gas. However, there exists both an attractive and a repulsive energy branch, which are symmetric about zero at unitarity [59], and when $T \gg T_F$, their contributions to the shift cancel [32, 44, 60]. As to the interpretation of the peak shift at degenerate temperatures, a solution to the Cooper problem in the presence of a $T > 0$ Fermi sea shows that it is energetically favorable to form pairs when $T \lesssim 0.5\, T_F$ [39], and the resulting pair energy agrees qualitatively with the observed shifts (grey line in Fig. 1(b)). However, it is known that fluctuations suppress the onset of pair condensation and superfluidity to $0.167(13)\, T_F$ [5, 11, 14, 61]. In a zero-temperature superfluid, BCS theory would predict a peak shift given by the pair binding energy $E_B = \Delta^2 / 2E_F$, where Δ is the pairing gap [3]. Including Hartree terms is found to result in an additional shift of the peak [27, 54].

We now turn to the widths, Γ, defined as the full width at half maximum of the rf spectra (see Fig. 1(c)). As the gas is cooled from the Boltzmann regime, the width gradually increases, and attains a maximum of $\Gamma = 1.35(5)\, E_F$ near $T = 0.44(4)\, T_F$. For temperatures much higher than T_F, the system is a Boltzmann gas of atoms scattering with a unitarity limited cross section $\sigma \sim \lambda_T^2$. Transport properties and short-range pair correlations are governed by the scattering rate $\Gamma = n_\downarrow \sigma \langle v_{\rm rel} \rangle \sim \hbar n_\downarrow \lambda_T / m$ and a mean-free path $l = (n_\downarrow \sigma)^{-1} \sim (n_\downarrow \lambda_T^2)^{-1}$, where $n_\downarrow$ is the density of atoms in $|\downarrow\rangle$, and $\langle v_{\rm rel} \rangle \sim \hbar / m \lambda_T$ is the thermally averaged relative velocity. This leads to a width that scales as $\Gamma \propto 1/\sqrt{T}$, shown as the dot-dashed line in Fig. 1(c) [32].

As the cloud is cooled below $T \approx 0.5\, T_F$, the width decreases linearly with temperature to $\Gamma \sim 0.52\, E_F / \hbar$ in the coldest gases measured ($T = 0.10(1)\, T_F$). For temperatures below T_c, we expect the gas to consist of pairs of size ξ. The rf spectrum will be broadened by the distribution of momenta $\sim \hbar / \xi$ inside each pair, leading to a spread of possible final kinetic energies $\hbar^2 k^2 / m \sim \hbar^2 / m \xi^2$ and a corresponding spectral width $\hbar / m \xi^2$. At unitarity and at $T = 0$, the pair size is set by the interparticle spacing λ_F [3, 5, 26]. Thus the rf width at low temperatures is $\Gamma \sim \hbar n \lambda_F / m$.

For temperatures above T_c, it has been suggested that the normal fluid can be described as a Fermi liquid [15, 62]. This would imply a quadratic relation between the peak width and the temperature [63], as observed in the widths of the rf spectra of Fermi polarons at unitarity [45]. However, the measured width of the spin-balanced Fermi gas changes linearly in temperature, implying non-Fermi liquid behavior in the normal fluid. In addition, $\Gamma > E_F / \hbar$ for $0.3 \lesssim T/T_F \lesssim 1.2$, indicating a breakdown of well-defined quasiparticles over a large range of temperatures near the quantum critical regime [10, 12, 13].

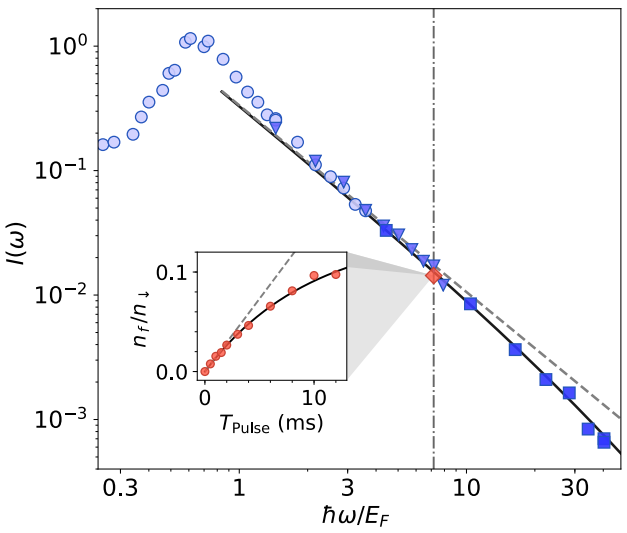

FIG. 2. Rf spectrum at high frequencies. Here, the temperature of the gas is $T/T_F = 0.10(1)$, the pulse duration is $T_{\rm Pulse} = 1$ ms, and the Rabi frequencies are $2\pi \times 536$ Hz (light blue circles), $2\pi \times 1.20$ kHz (medium blue triangles), and $2\pi \times 3.04$ kHz (dark blue squares). The black solid line shows a fit of Eq. 1 to the data, while the grey dashed line shows the fit neglecting final state interactions. The contact can be directly obtained from the transfer rate at a fixed detuning of 60 kHz ($\hbar\omega/E_F \sim 7.1$) (dot-dashed vertical line). Inset: we vary the pulse time at this fixed detuning, and extract the initial slope (dashed line) of the exponential saturating fit (solid line). The rf transfer rate obtained from the initial linear slope is shown as the red diamond in the main plot. Here, $\Omega_R = 2\pi \times 1.18$ kHz.

We now consider the rf spectrum at frequencies much larger than $E_F/\hbar$, where the rf-coupled high-momentum tails reveal information about the short-range pair correlations between atoms. In a gas with contact interactions, the pair correlation function at short distances is $\lim_{r \to 0} \langle n_\uparrow(\mathbf{r_0} + \mathbf{r}/\mathbf{2}) n_\downarrow(\mathbf{r_0} - \mathbf{r}/\mathbf{2}) \rangle = C/(4\pi r)^2$. The contact C connects a number of fundamental relations, independent of the details of the short-range interaction potential [28]. In particular, the contact governs the momentum distribution at large momenta: $\lim_{k \to \infty} n(k) = C/k^4$. For rf spectroscopy, the density of final states scales as $\sqrt{\omega}$, and the energy cost to flip a spin at high momenta is $\lim_{k \to \infty} \hbar\omega = \hbar^2 k^2 / m$. Thus, the number of atoms transferred by the rf pulse at high frequencies in linear response is $\propto C/\omega^{3/2}$ [5, 27]. Including final state interactions, the general expression for the rf transfer rate in a gas with unitarity-limited initial state interactions is [64]:

$$\lim_{\omega \to \infty} I(\omega) = \left(\frac{C}{N k_{\rm F}} \right) \frac{1}{2\sqrt{2}\pi\,(1 + \hbar\omega/E_b)} \left(\frac{E_{\rm F}}{\hbar\omega} \right)^{3/2}, \quad (1)$$

where $N = N_\uparrow + N_\downarrow$ is the total number of atoms, and the final state molecular binding energy is

$E_b = \hbar^2/ma_f^2 \approx h \times 433$ kHz $\approx 40\,E_F$. Fig. 2 shows a typical rf spectrum at $T/T_F = 0.10$, with a fit of Eq. 1 to data with detunings $\hbar\omega > 3\,E_F$, using the dimensionless contact $\tilde{C} = C/Nk_F$ as the only free parameter. At detunings larger than about 10 E_F, the data deviates from a typical $\omega^{-3/2}$ tail, and is better described by the full expression Eq. 1 including final state interactions. Here, the Rabi frequency was varied across the plot to ensure small transfers near the peak and a high signal-to-noise ratio at detunings up to $\hbar\omega/E_F = 31$. The fit of Eq. 1 to the data gives a low-temperature contact of $\tilde{C} = 3.07(6)$, consistent with a quantum Monte-Carlo result $\tilde{C} = 2.95(10)$ [65], the Luttinger-Ward (L-W) calculation $\tilde{C} = 3.02$ [27], as well as previous measurements using losses $\tilde{C} = 3.1(3)$ [66] and Bragg spectroscopy $\tilde{C} = 3.06(8)$ [53].

For a more efficient measurement of the contact across a range of temperatures, we vary the pulse time at a fixed detuning of 60 kHz ($\hbar\omega/E_F \gtrsim 6$) that is large compared to the Fermi energy and temperature. [39]. Deviations from linear response are observed for transfers as small as 5% (see inset of Fig. 2). We fit the transfers to an exponentially saturating function $A(1-\exp(-T_{\rm Pulse}/\tau))$, and find the initial linear slope A/τ in order to extract the contact for each temperature using Eq. 1. This ensures that every measurement is taken in the linear response regime.

In Fig. 3(a), we show the temperature dependence of the contact. As the gas is cooled, the contact shows a gradual increase down to the superfluid transition T_c. Entering the superfluid transition, the contact rapidly rises by approximately 15%. The changes in the contact reveal the temperature dependence of short-range pair correlations in the spin-balanced Fermi gas. At temperatures far above T_F, the contact reflects the inverse mean free path in the gas $1/l \sim 1/T$. At lower temperatures, the behavior of the contact is better described by a third-order virial expansion (see inset of 3(a)) [36]. Near T_c, predictions of the contact vary considerably. In the quantum critical regime, a leading-order 1/N calculation (equivalent to a Gaussian pair fluctuation or Nozières–Schmitt-Rink method) results in a prediction $\tilde{C}(\mu = 0, T \approx 0.68\ T_F) = 2.34$ [10], which is consistent with our measurement of $\tilde{C}(T = 0.65(4)\ T_F) = 2.29(13)$. For temperatures above the superfluid transition, our data agree well with both a bold diagrammatic Monte Carlo calculation [38], and, especially near T_c, the L-W calculation [32]. The contact rises as the temperature is decreased below T_c, a feature captured by the L-W formalism, in which the contact is directly sensitive to pairing: $\tilde{C} \sim (\Delta/E_F)^2$ [27, 33]. While short-range pair correlations do not necessarily signify pairing [35], the rapid rise of the contact below T_c is strongly indicative of an additional contribution from fermion pairs, as predicted by L-W. At temperatures $T \ll T_c$, below the reach of our experiment, phonons are likely the only remaining excitations in the unitary Fermi gas, and are expected to contribute to the contact by an amount that scales as T^4 [67].

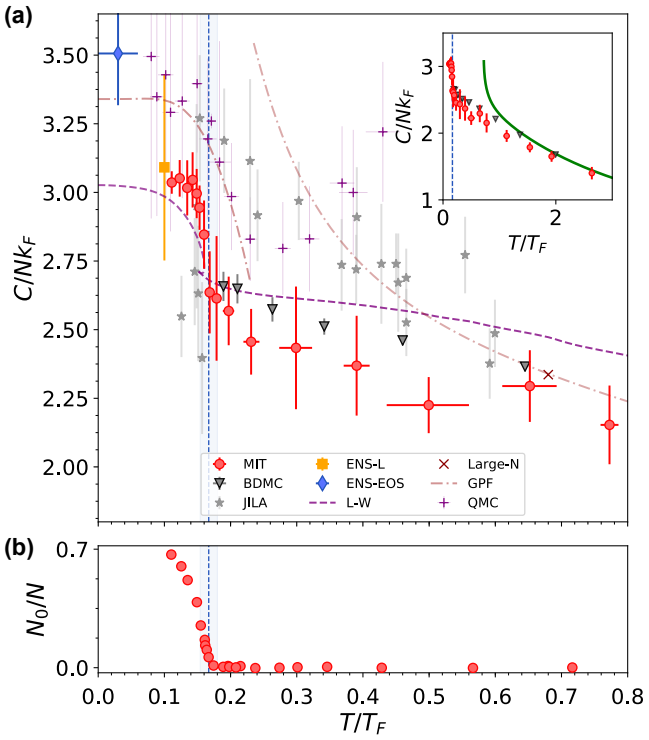

FIG. 3. The dimensionless contact C/Nk_F (a) and condensate fraction N_0/N (b) of the unitary Fermi gas as a function of the reduced temperature T/T_F. Our measurements of the contact (red points) are compared with a number of theoretical estimates: Bold-Diagrammatic Monte Carlo (BDMC) [38], QMC [37], Luttinger-Ward (L-W) [32], Large-N [10], and Gaussian pair fluctuations (GPF) [36]. Also shown is the homogeneous contact obtained from the equation of state (ENS-EOS) [62], from loss rate measurements (ENS-L) [66], and from rf spectroscopy by the JILA group [18] across a range of temperatures. The vertical blue dotted lines and light blue shaded vertical regions mark $T_c/T_F = 0.167(13)$ [14]. The inset of (a) shows the contact over a wider range of temperatures and marks the high-temperature agreement with the 3rd order virial expansion. The error bars account for the statistical uncertainties in the data.

In conclusion, rf spectroscopy of the homogeneous unitary Fermi gas reveals strong attractive interactions, the non-Fermi-liquid nature of excitations in the gas across the quantum critical regime, and a rapid increase in short-range pair correlations upon entering the superfluid regime. The strong variation with temperature of the position of the spectral peak may serve as a local thermometer in future studies of heat transport in ultracold Fermi gases. Furthermore, these measurements of the contact provide a benchmark for many-body theories of the unitary Fermi gas. The uniform trap enables direct access to homogeneous measurements of thermodynamic quantities, and increases sensitivity to abrupt changes

of those quantities near phase transitions. This could be particularly useful in the limit of high spin imbalance, where the nature of impurities suddenly transitions from Fermi polarons to molecules. [68, 69].

We note that measurements of the temperature dependence of the contact were simultaneously performed at Swinburne using Bragg spectroscopy. Their data are in excellent agreement with the present results.

We thank C. J. Vale, F. Werner, and W. Zwerger for helpful discussions. This work was supported by the NSF, AFOSR, ONR, the AFOSR MURI on Exotic Phases, and the David and Lucile Packard Foundation. J.S. was supported by LabEX ENS-ICFP: ANR-10-LABX-0010/ANR-10-IDEX-0001-02 PSL*.

[1] Hen *et al.*, Science **346**, 614 (2014).
[2] R. Weiss, B. Bazak, and N. Barnea, Phys. Rev. Lett. **114**, 012501 (2015).
[3] W. Ketterle and M. W. Zwierlein, *Ultra-cold Fermi Gases, Proceedings of the International School of Physics Enrico Fermi, Course CLXIV, Varenna 2006*, edited by M. Inguscio, W. Ketterle, and C. Salomon (IOS Press, Amsterdam, 2008) pp. 247–422.
[4] S. Giorgini, L. P. Pitaevskii, and S. Stringari, Rev. Mod. Phys. **80**, 1215 (2008).
[5] W. Zwerger, *Proceedings of the International School of Physics "Enrico Fermi" - Course 191 "Quantum Matter at Ultralow Temperatures"*, edited by M. Inguscio, W. Ketterle, S. Stringari, and G. Roati (IOS Press, Amsterdam; SIF Bologna, 2016) pp. 63–142.
[6] M. W. Zwierlein, in *Novel Superfluids* (Oxford University Press, 2014) pp. 269–422.
[7] A. J. Leggett, Phys. Rev. Lett. **29**, 1227 (1972).
[8] P. A. Lee, N. Nagaosa, and X.-G. Wen, Rev. Mod. Phys. **78**, 17 (2006).
[9] G. Baym, C. Pethick, and D. Pines, Nature **224**, 673 (1969).
[10] T. Enss, Phys. Rev. A **86**, 013616 (2012).
[11] M. Randeria and E. Taylor, Annual Review of Condensed Matter Physics **5**, 209 (2014).
[12] P. Nikolic and S. Sachdev, Phys. Rev. A **75**, 033608 (2007).
[13] B. Frank, J. Lang, and W. Zwerger, JETP **127**, 812 (2018).
[14] M. J. H. Ku, A. T. Sommer, L. W. Cheuk, and M. W. Zwierlein, Science **335**, 563 (2012).
[15] S. Nascimbène, N. Navon, S. Pilati, F. Chevy, S. Giorgini, A. Georges, and C. Salomon, Phys. Rev. Lett. **106**, 215303 (2011).
[16] I. Z. Rothstein and P. Shrivastava, Phys. Rev. B **99**, 035101 (2019).
[17] J. P. Gaebler, J. T. Stewart, T. E. Drake, D. S. Jin, A. Perali, P. Pieri, and G. C. Strinati, Nature Physics **6**, 569 (2010).
[18] Y. Sagi, T. E. Drake, R. Paudel, R. Chapurin, and D. S. Jin, Phys. Rev. Lett. **114**, 075301 (2015).
[19] A. Perali, P. Pieri, G.C. Strinati, and C. Castellani, Phys. Rev. B **66**, 024510 (2002).
[20] H. Hu, X. J. Liu, P. D. Drummond, and H. Dong, Phys. Rev. Lett. **104**, 240407 (2010).
[21] P. Magierski, G. Wlazłowski, and A. Bulgac, Phys. Rev. Lett. **107**, 145304 (2011).
[22] S. Gupta, Z. Hadzibabic, M. W. Zwierlein, C. A. Stan, K. Dieckmann, C. H. Schunck, E. G. Van Kempen, B. J. Verhaar, and W. Ketterle, Science **300**, 1723 (2003).
[23] C. A. Regal and D. S. Jin, Phys. Rev. Lett. **90**, 230404 (2003).
[24] C. A. Regal, C. Ticknor, J. L. Bohn, and D. S. Jin, Nature **424**, 47 (2003).
[25] C. Chin, M. Bartenstein, A. Altmeyer, S. Riedl, S. Jochim, J. Denschlag, and R. Grimm, Science **305**, 1128 (2004).
[26] C. H. Schunck, Y.-I. Shin, A. Schirotzek, and W. Ketterle, Nature **454**, 739 (2008).
[27] R. Haussmann, M. Punk, and W. Zwerger, Phys. Rev. A **80**, 063612 (2009).
[28] S. Tan, Annals of Physics **323**, 2971 (2008).
[29] S. Tan, Annals of Physics **323**, 2952 (2008).
[30] S. Tan, Annals of Physics **323**, 2987 (2008).
[31] E. Taylor and M. Randeria, Phys. Rev. A **81**, 53610 (2010).
[32] T. Enss, R. Haussmann, and W. Zwerger, Annals of Physics **326**, 770 (2011).
[33] P. Pieri, A. Perali, and G. C. Strinati, Nature Physics **5**, 736 (2009).
[34] F. Palestini, A. Perali, P. Pieri, and G. C. Strinati, Phys. Rev. A **82**, 021605(R) (2010).
[35] E. J. Mueller, Reports on Progress in Physics **80**, 104401 (2017).
[36] H. Hu, X. J. Liu, and P. D. Drummond, New Journal of Physics **13**, 035007 (2011).
[37] O. Goulko and M. Wingate, Phys. Rev. A **93**, 053604 (2016).
[38] R. Rossi, T. Ohgoe, E. Kozik, N. Prokof'ev, B. Svistunov, K. Van Houcke, and F. Werner, Phys. Rev. Lett. **121**, 130406 (2018).
[39] See Supplemental Material [url] for further information, which includes Refs. [40–43].
[40] L. N. Cooper, Phys. Rev. **104**, 1189 (1956).
[41] M. Y. Veillette, D. E. Sheehy, and L. Radzihovsky, Phys. Rev. A **75**, 043614 (2007).
[42] L. Pisani, P. Pieri, and G. C. Strinati, Phys. Rev. B **98**, 104507 (2018).
[43] M. Naraschewski and D. M. Stamper-Kurn, Phys. Rev. A **58**, 2423 (1998).
[44] M. Sun and X. Leyronas, Phys. Rev. A **92**, 53611 (2015).
[45] Z. Yan, P. B. Patel, B. Mukherjee, R. J. Fletcher, J. Struck, and M. W. Zwierlein, (2018), arXiv:1811.00481.
[46] C. H. Schunck, Y. Shin, A. Schirotzek, M. W. Zwierlein, and W. Ketterle, Science **316**, 867 (2007).
[47] G. Baym, C. J. Pethick, Z. Yu, and M. W. Zwierlein, Phys. Rev. Lett. **99**, 190407 (2007).
[48] M. Punk and W. Zwerger, Phys. Rev. Lett. **99**, 170404 (2007).
[49] J. T. Stewart, J. P. Gaebler, T. E. Drake, and D. S. Jin, Phys. Rev. Lett. **104**, 235301 (2010).
[50] C. Shkedrov, Y. Florshaim, G. Ness, A. Gandman, and Y. Sagi, Phys. Rev. Lett. **121**, 093402 (2018).
[51] E. D. Kuhnle, H. Hu, X. J. Liu, P. Dyke, M. Mark, P. D. Drummond, P. Hannaford, and C. J. Vale, Phys. Rev. Lett. **105**, 070402 (2010).

[52] E. D. Kuhnle, S. Hoinka, P. Dyke, H. Hu, P. Hannaford, and C. J. Vale, Phys. Rev. Lett. **106**, 170402 (2011).
[53] S. Hoinka, M. Lingham, K. Fenech, H. Hu, C. J. Vale, J. E. Drut, and S. Gandolfi, Phys. Rev. Lett. **110**, 055305 (2013).
[54] A. Schirotzek, Y.-I. Shin, C. H. Schunck, and W. Ketterle, Phys. Rev. Lett. **101**, 140403 (2008).
[55] Y. Sagi, T. E. Drake, R. Paudel, and D. S. Jin, Phys. Rev. Lett. **109**, 220402 (2012).
[56] A. L. Gaunt, T. F. Schmidutz, I. Gotlibovych, R. P. Smith, and Z. Hadzibabic, Phys. Rev. Lett. **110**, 200406 (2013).
[57] B. Mukherjee, Z. Yan, P. B. Patel, Z. Hadzibabic, T. Yefsah, J. Struck, and M. W. Zwierlein, Phys. Rev. Lett. **118**, 123401 (2017).
[58] K. Hueck, N. Luick, L. Sobirey, J. Siegl, T. Lompe, and H. Moritz, Phys. Rev. Lett. **120**, 60402 (2018).
[59] T.-L. Ho and E. J. Mueller, Phys. Rev. Lett. **92**, 160404 (2004).
[60] R. J. Fletcher, R. Lopes, J. Man, N. Navon, R. P. Smith, M. W. Zwierlein, and Z. Hadzibabic, Science **355**, 377 (2017).
[61] P. Nozières and S. Schmitt-Rink, Journal of Low Temperature Physics **59**, 195 (1985).
[62] S. Nascimbène, N. Navon, K. J. Jiang, F. Chevy, and C. Salomon, Nature **463**, 1057 (2010).
[63] P. Nozieres and D. Pines, *The Theory of Quantum Liquids, Vol I: Normal Fermi Liquids*, 1st ed. (W.A. Benjamin, New York, 1966).
[64] E. Braaten, D. Kang, and L. Platter, Phys. Rev. Lett. **104**, 223004 (2010).
[65] J. E. Drut, T. A. Lähde, and T. Ten, Phys. Rev. Lett. **106**, 205302 (2011).
[66] S. Laurent, M. Pierce, M. Delehaye, T. Yefsah, F. Chevy, and C. Salomon, Phys. Rev. Lett. **118**, 103403 (2017).
[67] Z. Yu, G. M. Bruun, and G. Baym, Phys. Rev. A **80**, 023615 (2009).
[68] M. Punk, P. T. Dumitrescu, and W. Zwerger, Phys. Rev. A **80**, 053605 (2009).
[69] A. Schirotzek, C.-H. Wu, A. Sommer, and M. W. Zwierlein, Phys. Rev. Lett. **102**, 230402 (2009).